A PENALTY MODEL FOR THE ANALYSIS OF LAMINATED COMPOSITE SHELLS

F. FRATERNALI

University of Salerno, Fisciano (Salerno) 84084, Italy

and

J. N. REDDY

Texas A&M University, College Station, Texas 77843, U.S.A.

Abstract—A theory for laminated composite shells and a finite element model based on this theory are presented. Due to a flexible layer-wise description of the displacement field, the theory accounts for an accurate description of the shear deformation and the stretching of transverse normals to the middle surface. With respect to other layer-wise theories which are available in the literature, the present one distinguishes itself by the use of the penalty method to enforce the perfect bonding between adjacent layers. This method offers the possibility to easily obtain accurate interlaminar stresses. Numerical results for simply supported laminated spherical shells are presented to show the features of the proposed theory and its accuracy.

NOMENCLATURE

Ω	middle surface of the laminated shell (Fig. 1)
θ_1, θ_2	coordinates along the lines of curvature of Ω
$l_1(\theta_2), l_2(\theta_1)$	lengths of the lines of curvature of Ω (Fig. 1)
ζ	coordinate normal to Ω
R_1, R_2	principal radii of curvature of Ω
h	total thickness of the laminated shell (Fig. 1)
a_1^2, a_2^2	coefficients of the first fundamental form of Ω
N	number of layers composing the laminated shell (Fig. 1)
$\Omega^{(K)}$	middle surface of the Kth layer
$\theta_1^{(K)}, \theta_2^{(K)}$	coordinates along the lines of curvature of $\Omega^{(K)}$
$\zeta^{(K)}$	coordinate normal to $\Omega^{(K)}$
$\hat{e}_1^{(K)}, \hat{e}_2^{(K)}$	unit vectors tangent to the $\theta_1^{(K)}$ and $\theta_2^{(K)}$ lines
$\hat{n}^{(K)}$	unit vector normal to $\Omega^{(K)}$
$R_1^{(K)}, R_2^{(K)}$	principal radii of curvature of $\Omega^{(K)}$
$h^{(K)}$	thickness of the Kth layer (Fig. 1)
$d^{(K)}$	ζ-coordinate of the points of $\Omega^{(K)}$
$(a_1^{(K)})^2, (a_2^{(K)})^2$	coefficients of the first fundamental form of $\Omega^{(K)}$
$\mathbf{p}^+, \mathbf{p}^-$	surface forces applied on the bottom surface (S^+) and on the top surface (S^-) of the laminated shell.

Roman lower case subscripts (e.g. i, j) are assumed to range over integers $1, 2, 3$, while Greek lower case subscripts (e.g. α, β) are assumed to range over the integers $1, 2$. The range of the capital subscripts and superscripts will be explicitly stated in the text.

1. INTRODUCTION

The increasing use of laminated composite structures in several engineering applications has generated considerable interest among many researchers to formulate refined theories for the analysis of such structures. A majority of these theories deals with laminated composite plates, while a more restricted number of theories have been proposed for laminated composite beams and shells. In the context of the displacements based theories, we can identify two different categories of formulations. The first category consists of formulations which model the laminated structure as an equivalent single layer structure and use the kinematic assumptions of the classical theory of beams, plate or shells or a suitable refinement of them (see, for example, Christensen et al., 1977; Murthy, 1981; Reddy, 1984a, b, c; Reddy and Liu, 1985; Reddy and Chandrasekhara, 1987; Bhimarradi et al., 1989; Ascione and Fraternali, 1990). The second category of theories assumes that

the thickness approximation of the displacements field can be accomplished via a piecewise approximation through each individual lamina (layer-wise theories). This kind of formulation was introduced by Reddy (1987) for laminated composite plates and extended to laminated composite cylindrical shells by Reddy and Barbero (1990). Similar theories have appeared in the literature (Sreenivas, 1973; Murakami, 1984; Hinrichsen and Palazzotto, 1986; Yuan and Miller, 1989; Tralli et al., 1990; Ascione and Fraternali, 1992).

The major difference between the above two categories is that layer-wise theories model inplane and transverse shear deformations in a more accurate way. Furthermore, they offer the possibility to compute interlaminar stresses (Reddy et al., 1989), which cannot be predicted in an efficient way by a single layer theory, since it does not allow for possible discontinuities in strains at an interface of dissimilar layers.

This study presents an original theory of laminated shells. The theory is based on the following fundamental assumptions: (a) the displacement field can be chosen independently in each individual layer, like in the layer-wise theory of Reddy (1987); (b) the layers are perfectly bonded one to another and the bonding constraint is imposed via penalty method. From a mechanical point of view, the penalty method is equivalent to the introduction of an auxiliary model (penalty model), in which the layers are connected by radial and transverse springs. Letting the stiffness of such springs have a large value, it is possible to achieve perfect bonding between layers. A similar theory was proposed by Ascione and Fraternali (1992) for the analysis of laminated curved beams. Alternatively to the penalty method, two other techniques can be utilized to enforce the bonding constraint between layers. The first consists of using constraint equations to reduce the number of independent kinematical variables (Reddy, 1987); the second consists of the Lagrange multiplier method. This last method leads one to identify the interlaminar (tangential and radial) stresses as the Lagrange multipliers and to formulate a theory in which these quantities are independent variables as well as the generalized displacements of the layers. Differently, the first technique compels one to post-process the results in terms of displacements, via equilibrium equations, to obtain interlaminar stresses (Reddy et al., 1989). It can be shown (see, for example, Malkus and Hughes, 1978; Carey and Oden, 1983; Reddy, 1992a, b) that the penalty method proposed in this work produces an approximation of the interlaminar stresses, which can be identified with the reactions of the springs interposed between layers in the penalty model. The advantage of the penalty method consists of the possibility to easily compute accurate interlaminar stresses, without assuming them as additional independent variables or using the equilibrium equations.

Besides that for the computation of displacements and interlaminar stresses, the theory proposed in this study can be used to evaluate stress distribution within the different layers of a laminated shell. Indeed, once displacements and interlaminar stresses have been computed, it is possible to derive inplane stresses directly from the constitutive equations and transverse stresses by post-processing the results via equilibrium equations (see Section 3).

To verify the accuracy of the theory proposed, the present study also contains a finite element approximation of the theory and some numerical results for laminated spherical shells. These results are compared with those obtained by Reddy (1984c) and by Reddy et al. (1989).

2. FORMULATION

2.1. Kinematical assumption

Let us consider a shell made up of N orthotropic layers (Fig. 1). We assume that the displacement field of the generic layer, say the Kth one,

$$\mathbf{u}^{(K)} = u_\alpha^{(K)}(\theta_\alpha^{(K)}, \zeta^{(K)})\hat{\mathbf{e}}_\alpha^{(K)} + u_3^{(K)}(\theta_\alpha^{(K)}, \zeta^{(K)})\hat{\mathbf{n}}^{(K)}, \tag{1}$$

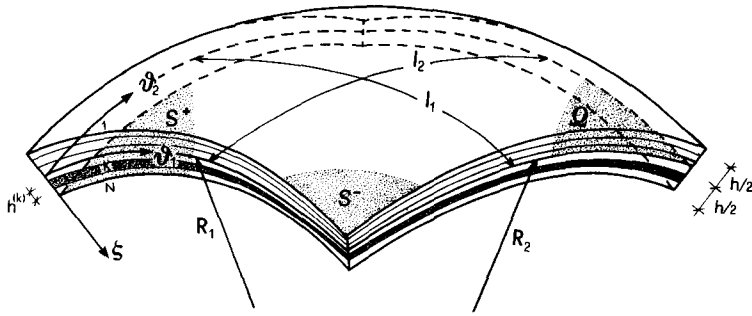can be expanded as a suitable function of powers of the thickness coordinates $\zeta^{(K)}$:

Fig. 1. Laminated composite shell.

$$u_\alpha^{(K)}(\theta_\alpha^{(K)}, \zeta^{(K)}) = v_\alpha^{(K)}(\theta_\alpha^{(K)}) + \sum_{P=1}^{A^{(K)}} \frac{(\zeta^{(K)})^P}{P!} \, \phi_{P\alpha}^{(K)}(\theta_\alpha^{(K)}), \tag{2a}$$

$$u_3^{(K)}(\theta_\alpha^{(K)}, \zeta^{(K)}) = v_3^{(K)}(\theta_\alpha^{(K)}) + \sum_{Q=1}^{B^{(K)}} \frac{(\zeta^{(K)})^Q}{Q!} \, \phi_{Q3}^{(K)}(\theta_\alpha^{(K)}), \tag{2b}$$

where

$$v_i^{(K)}(\theta_\alpha^{(K)}) = u_i^{(K)}(\theta_\alpha^{(K)}, 0), \tag{3a}$$

$$\phi_{Ri}^{(K)}(\theta_\alpha^{(K)}) = \frac{\partial^R u_i^{(K)}}{(\partial \zeta^{(K)})^R}\Bigg|_{(\theta_\alpha^{(K)}, 0)}. \tag{3b}$$

In developing the governing equations we leave unspecified the orders $A^{(K)}$ and $B^{(K)}$ of the series expansions in (2). These orders will be specified in the numerical applications in relation to the magnitude of the ratios thickness-to-length and thickness-to-radius. We set $C^{(K)} = \sup \{A^{(K)}, B^{(K)}\}$.

By setting $A^{(K)} = 1$ we obtain, for the layer under consideration, the first order shear deformation theory, while by setting $B^{(K)} \geqslant 1$ we account for a stretching of the normals to the middle surface. In particular, the case $A^{(K)} = B^{(K)} = 2$ corresponds to the Hildebrand, Reissner and Thomas theory (1949); the case $A^{(K)} = 1$, $B^{(K)} = 2$ corresponds to the theory of Naghdi (1957).

By making use of eqn (1), we obtain the following expansion of the displacement gradient:

$$\nabla u^{(K)} \hat{e}_\alpha^{(K)} = \frac{1}{(1 - \zeta^{(K)}/R_\alpha^{(K)})} \left(\mathbf{l}_\alpha^{(K)} + \sum_{R=1}^{C^{(K)}} \mathbf{d}_{R\alpha}^{(K)} \right) \quad \text{(no sum on } \alpha\text{)}, \tag{4a}$$

$$\nabla u^{(K)} \hat{n}^{(K)} = \mathbf{l}_3^{(K)} + \sum_{S=1}^{C^{(K)}-1} \mathbf{d}_{S3}^{(K)}, \tag{4b}$$

where

$$\mathbf{l}_\alpha^{(K)} = \frac{1}{a_\alpha^{(K)}} \frac{\partial \mathbf{v}^{(K)}}{\partial \theta_\alpha^{(K)}}, \quad \mathbf{l}_3^{(K)} = \phi_1^{(K)}, \tag{5a, b}$$

$$\mathbf{d}_{R\alpha}^{(K)} = \frac{1}{a_\alpha^{(K)}} \frac{\partial \phi_R^{(K)}}{\partial \theta_\alpha^{(K)}} \quad R = 1, \ldots, C^{(K)}, \quad \mathbf{d}_{S3}^{(K)} = \phi_{S+1}^{(K)} \quad S = 1, \ldots, C^{(K)} - 1. \tag{6a, b}$$

$\mathbf{v}^{(K)}$ being the vector collecting $v_1^{(K)}$, $v_2^{(K)}$, $v_3^{(K)}$ and $\phi_T^{(K)}$ the vector collecting $\phi_{T1}^{(K)}$, $\phi_{T2}^{(K)}$, $\phi_{T3}^{(K)}$.

Making use of the formulae for the derivatives of $\hat{e}_1^{(K)}$, $\hat{e}_2^{(K)}$ (see, for example, Naghdi, 1972; Dym, 1974), we obtain the following expressions of the components of the vectors defined by eqns (5)–(6) with respect to $\hat{e}_\alpha^{(K)}$, $\hat{n}^{(K)}$:

$$\{l_1^{(K)}\} = \left\{ \begin{array}{c} \dfrac{1}{a_1^{(K)}} \dfrac{\partial v_1^{(K)}}{\partial \theta_1^{(K)}} + \dfrac{v_2^{(K)}}{a_1^{(K)} a_2^{(K)}} \dfrac{\partial a_1^{(K)}}{\partial \theta_2^{(K)}} - \dfrac{v_3^{(K)}}{R_1^{(K)}} \\[3mm] \dfrac{1}{a_1^{(K)}} \dfrac{\partial v_2^{(K)}}{\partial \theta_1^{(K)}} - \dfrac{v_1^{(K)}}{a_1^{(K)} a_2^{(K)}} \dfrac{\partial a_1^{(K)}}{\partial \theta_2^{(K)}} \\[3mm] \dfrac{1}{a_1^{(K)}} \dfrac{\partial v_3^{(K)}}{\partial \theta_1^{(K)}} + \dfrac{v_1^{(K)}}{R_1^{(K)}} \end{array} \right\}, \tag{7a}$$

$$\{l_2^{(K)}\} = \left\{ \begin{array}{c} \dfrac{1}{a_2^{(K)}} \dfrac{\partial v_1^{(K)}}{\partial \theta_2^{(K)}} - \dfrac{v_2^{(K)}}{a_1^{(K)} a_2^{(K)}} \dfrac{\partial a_2^{(K)}}{\partial \theta_1^{(K)}} \\[3mm] \dfrac{1}{a_2^{(K)}} \dfrac{\partial v_2^{(K)}}{\partial \theta_2^{(K)}} + \dfrac{v_1^{(K)}}{a_1^{(K)} a_2^{(K)}} \dfrac{\partial a_2^{(K)}}{\partial \theta_1^{(K)}} - \dfrac{v_3^{(K)}}{R_2^{(K)}} \\[3mm] \dfrac{1}{a_2^{(K)}} \dfrac{\partial v_3^{(K)}}{\partial \theta_2^{(K)}} + \dfrac{v_2^{(K)}}{R_2^{(K)}} \end{array} \right\}, \tag{7b}$$

$$\{l_3^{(K)}\} = \left\{ \begin{array}{c} \phi_{11}^{(K)} \\ \phi_{12}^{(K)} \\ \phi_{13}^{(K)} \end{array} \right\}, \tag{7c}$$

$$\{d_{R1}^{(K)}\} = \left\{ \begin{array}{c} \dfrac{1}{a_1^{(K)}} \dfrac{\partial \phi_{R1}^{(K)}}{\partial \theta_1^{(K)}} + \dfrac{\phi_{R2}^{(K)}}{a_1^{(K)} a_2^{(K)}} \dfrac{\partial a_1^{(K)}}{\partial \theta_2^{(K)}} - \dfrac{\phi_{R3}^{(K)}}{R_1^{(K)}} \\[3mm] \dfrac{1}{a_1^{(K)}} \dfrac{\partial \phi_{R2}^{(K)}}{\partial \theta_1^{(K)}} - \dfrac{\phi_{R1}^{(K)}}{a_1^{(K)} a_2^{(K)}} \dfrac{\partial a_1^{(K)}}{\partial \theta_2^{(K)}} \\[3mm] \dfrac{1}{a_1^{(K)}} \dfrac{\partial \phi_{R3}^{(K)}}{\partial \theta_1^{(K)}} + \dfrac{\phi_{R1}^{(K)}}{R_1^{(K)}} \end{array} \right\} \quad R = 1, \ldots, C^{(K)}, \tag{8a}$$

$$\{d_{R2}^{(K)}\} = \left\{ \begin{array}{c} \dfrac{1}{a_2^{(K)}} \dfrac{\partial \phi_{R1}^{(K)}}{\partial \theta_2^{(K)}} - \dfrac{\phi_{R2}^{(K)}}{a_1^{(K)} a_2^{(K)}} \dfrac{\partial a_2^{(K)}}{\partial \theta_1^{(K)}} \\[3mm] \dfrac{1}{a_2^{(K)}} \dfrac{\partial \phi_{R2}^{(K)}}{\partial \theta_2^{(K)}} + \dfrac{\phi_{R1}^{(K)}}{a_1^{(K)} a_2^{(K)}} \dfrac{\partial a_2^{(K)}}{\partial \theta_1^{(K)}} - \dfrac{\phi_{R3}^{(K)}}{R_2^{(K)}} \\[3mm] \dfrac{1}{a_2^{(K)}} \dfrac{\partial \phi_{R3}^{(K)}}{\partial \theta_2^{(K)}} + \dfrac{\phi_{R2}^{(K)}}{R_2^{(K)}} \end{array} \right\} \quad R = 1, \ldots, C^{(K)}, \tag{8b}$$

$$\{d_{S3}^{(K)}\} = \left\{ \begin{array}{c} \phi_{S+1,1}^{(K)} \\ \phi_{S+1,2}^{(K)} \\ \phi_{S+1,3}^{(K)} \end{array} \right\} \quad S = 1, \ldots, C^{(K)} - 1. \tag{8c}$$

It is understood that in eqns (8) the quantities $\phi_{P\alpha}^{(K)}$ have to be considered only if $P \leqslant A^{(K)}$, while the quantities $\phi_{Q3}^{(K)}$ have to be considered only if $Q \leqslant B^{(K)}$.

We assume that each layer is perfectly bonded to the adjacent ones, so that the following conditions hold:

$$\Delta \mathbf{u}^{(K)} = \mathbf{u}^{(K)} \left(\theta_\alpha, \zeta^{(K)} = \frac{h^{(K)}}{2} \right) - \mathbf{u}^{(K+1)} \left(\theta_\alpha, \zeta^{(K+1)} = -\frac{h^{(K+1)}}{2} \right) = 0 \quad K = 1, 2, \ldots, N-1. \tag{9}$$

2.2. Equilibrium equations

We derive the equilibrium equations using the principle of virtual displacements. It can be verified that the introduction of eqns (4) into the virtual work expression leads to the following equation:

$$\int_\Omega \left\{ \sum_{K=1}^N [\mathbf{N}_1^{(K)} \cdot \delta \mathbf{I}_1^{(K)} + \mathbf{N}_2^{(K)} \cdot \delta \mathbf{I}_2^{(K)} + \mathbf{N}_3^{(K)} \cdot \delta \mathbf{I}_3^{(K)} + \sum_{R=1}^{C^{(K)}} (\mathbf{M}_{R1}^{(K)} \cdot \delta \mathbf{d}_{R1}^{(K)} + \mathbf{M}_{R2}^{(K)} \cdot \delta \mathbf{d}_{R2}^{(K)}) \right.$$

$$\left. + \sum_{S=1}^{C^{(K)}-1} \mathbf{M}_{S3}^{(K)} \cdot \delta \mathbf{d}_{S3}^{(K)} \right] \left(1 - \frac{d^{(K)}}{R_1} \right) \left(1 - \frac{d^{(K)}}{R_2} \right) \right\} a_1 a_2 \, d\theta_1 \, d\theta_2$$

$$= \int_\Omega \mathbf{p}^- \cdot \left[\delta \mathbf{v}^{(1)} + \sum_{R=1}^{C^{(1)}} \frac{(-h^{(1)}/2)^R}{R!} \delta \phi_R^{(1)} \right] \left(1 + \frac{h^{(1)}}{2R_1} \right) \left(1 + \frac{h^{(1)}}{2R_2} \right) a_1 a_2 \, d\theta_1 \, d\theta_2$$

$$+ \int_\Omega \mathbf{p}^+ \cdot \left[\delta \mathbf{v}^{(N)} + \sum_{R=1}^{C^{(N)}} \frac{(h^{(N)}/2)^R}{R!} \delta \phi_R^{(N)} \right] \left(1 - \frac{h^{(N)}}{2R_1} \right) \left(1 - \frac{h^{(N)}}{2R_2} \right) a_1 a_2 \, d\theta_1 \, d\theta_2 \qquad (10)$$

where $\mathbf{N}_i^{(K)}$, $\mathbf{M}_{R\alpha}^{(K)}$, $\mathbf{M}_{S3}^{(K)}$ are the generalized stresses:

$$\mathbf{N}_\alpha^{(K)} = \int_{-h^{(K)}/2}^{h^{(K)}/2} \mathbf{t}_\alpha^{(K)} \left(1 - \frac{\zeta^{(K)}}{R_\beta^{(K)}} \right) d\zeta^{(K)} \quad (\alpha \neq \beta), \qquad (11a)$$

$$\mathbf{N}_3^{(K)} = \int_{-h^{(K)}/2}^{h^{(K)}/2} \mathbf{t}_3^{(K)} \left(1 - \frac{\zeta^{(K)}}{R_1^{(K)}} \right) \left(1 - \frac{\zeta^{(K)}}{R_2^{(K)}} \right) d\zeta^{(K)}, \qquad (11b)$$

$$\mathbf{M}_{R\alpha}^{(K)} = \int_{-h^{(K)}/2}^{h^{(K)}/2} \mathbf{t}_\alpha^{(K)} \frac{(\zeta^{(K)})^R}{R!} \left(1 - \frac{\zeta^{(K)}}{R_\beta^{(K)}} \right) d\zeta^{(K)} \quad (\alpha \neq \beta) \quad R = 1, \ldots, C^{(K)}, \qquad (12a)$$

$$\mathbf{M}_{S3}^{(K)} = \int_{-h^{(K)}/2}^{h^{(K)}/2} \mathbf{t}_3^{(K)} \frac{(\zeta^{(K)})^S}{S!} \left(1 - \frac{\zeta^{(K)}}{R_1^{(K)}} \right) \left(1 - \frac{\zeta^{(K)}}{R_2^{(K)}} \right) d\zeta^{(K)} \quad S = 1, \ldots, C^{(K)} - 1, \qquad (12b)$$

$\mathbf{t}_\alpha^{(K)}$ being the traction vector on the surface element of normal $\hat{\mathbf{e}}_\alpha^{(K)}$, and $\mathbf{t}_3^{(K)}$ the traction vector on the surface element of normal $\hat{\mathbf{n}}^{(K)}$.

In eqn (10) we have used the following relations:

$$d\Omega^{(K)} = a_1^{(K)} a_2^{(K)} \, d\theta_1^{(K)} \, d\theta_2^{(K)}, \qquad (13a)$$

$$dS^{(K)} = \left(1 - \frac{\zeta^{(K)}}{R_1^{(K)}} \right) \left(1 - \frac{\zeta^{(K)}}{R_2^{(K)}} \right) d\Omega^{(K)}, \qquad (13b)$$

$$dV^{(K)} = \left(1 - \frac{\zeta^{(K)}}{R_1^{(K)}} \right) \left(1 - \frac{\zeta^{(K)}}{R_2^{(K)}} \right) d\Omega^{(K)} \, d\zeta^{(K)}, \qquad (13c)$$

$$\frac{A_\alpha^{(K)}}{A_\alpha} \frac{d\theta_\alpha^{(K)}}{d\theta_\alpha} = \frac{R_\alpha^{(K)}}{R_\alpha} = \frac{R_\alpha - d^{(K)}}{R_\alpha} \quad \text{(no sum on } \alpha\text{)}, \qquad (13d)$$

which give the surface element of $\Omega^{(K)}$, the surface element at $\zeta^{(K)} = \text{const}$, the volume element of the Kth layer and the transformation between the two orthogonal curvilinear coordinates $\theta_\alpha^{(K)}$ and θ_α. The components of the generalized stresses with respect to $\hat{\mathbf{e}}_\alpha^{(K)}$, $\hat{\mathbf{n}}^{(K)}$ are given by:

$$\{N_1^{(K)}\} = \left\{ \begin{array}{c} \displaystyle\int_{-h^{(K)}/2}^{h^{(K)}/2} \sigma_{11}^{(K)} \left(1 - \frac{\zeta^{(K)}}{R_2^{(K)}} \right) d\zeta^{(K)} \\[2ex] \displaystyle\int_{-h^{(K)}/2}^{h^{(K)}/2} \sigma_{21}^{(K)} \left(1 - \frac{\zeta^{(K)}}{R_2^{(K)}} \right) d\zeta^{(K)} \\[2ex] \displaystyle\int_{-h^{(K)}/2}^{h^{(K)}/2} \sigma_{31}^{(K)} \left(1 - \frac{\zeta^{(K)}}{R_2^{(K)}} \right) d\zeta^{(K)} \end{array} \right\}, \qquad (14a)$$

$$
\{N_2^{(K)}\} = \left\{
\begin{array}{c}
\displaystyle\int_{-h^{(K)}/2}^{h^{(K)}/2} \sigma_{12}^{(K)}\left(1 - \frac{\zeta^{(K)}}{R_1^{(K)}}\right)\mathrm{d}\zeta^{(K)} \\[12pt]
\displaystyle\int_{-h^{(K)}/2}^{h^{(K)}/2} \sigma_{22}^{(K)}\left(1 - \frac{\zeta^{(K)}}{R_1^{(K)}}\right)\mathrm{d}\zeta^{(K)} \\[12pt]
\displaystyle\int_{-h^{(K)}/2}^{h^{(K)}/2} \sigma_{32}^{(K)}\left(1 - \frac{\zeta^{(K)}}{R_1^{(K)}}\right)\mathrm{d}\zeta^{(K)}
\end{array}
\right\}, \tag{14b}
$$

$$
\{N_3^{(K)}\} = \left\{
\begin{array}{c}
\displaystyle\int_{-h^{(K)}/2}^{h^{(K)}/2} \sigma_{13}^{(K)}\left(1 - \frac{\zeta^{(K)}}{R_1^{(K)}}\right)\left(1 - \frac{\zeta^{(K)}}{R_2^{(K)}}\right)\mathrm{d}\zeta^{(K)} \\[12pt]
\displaystyle\int_{-h^{(K)}/2}^{h^{(K)}/2} \sigma_{23}^{(K)}\left(1 - \frac{\zeta^{(K)}}{R_1^{(K)}}\right)\left(1 - \frac{\zeta^{(K)}}{R_2^{(K)}}\right)\mathrm{d}\zeta^{(K)} \\[12pt]
\displaystyle\int_{-h^{(K)}/2}^{h^{(K)}/2} \sigma_{33}^{(K)}\left(1 - \frac{\zeta^{(K)}}{R_1^{(K)}}\right)\left(1 - \frac{\zeta^{(K)}}{R_2^{(K)}}\right)\mathrm{d}\zeta^{(K)}
\end{array}
\right\}, \tag{14c}
$$

$$
\{M_{R1}^{(K)}\} = \left\{
\begin{array}{c}
\displaystyle\frac{1}{R!}\int_{-h^{(K)}/2}^{h^{(K)}/2} \sigma_{11}^{(K)}(\zeta^{(K)})^R\left(1 - \frac{\zeta^{(K)}}{R_2^{(K)}}\right)\mathrm{d}\zeta^{(K)} \\[12pt]
\displaystyle\frac{1}{R!}\int_{-h^{(K)}/2}^{h^{(K)}/2} \sigma_{21}^{(K)}(\zeta^{(K)})^R\left(1 - \frac{\zeta^{(K)}}{R_2^{(K)}}\right)\mathrm{d}\zeta^{(K)} \\[12pt]
\displaystyle\frac{1}{R!}\int_{-h^{(K)}/2}^{h^{(K)}/2} \sigma_{31}^{(K)}(\zeta^{(K)})^R\left(1 - \frac{\zeta^{(K)}}{R_2^{(K)}}\right)\mathrm{d}\zeta^{(K)}
\end{array}
\right\} \quad R = 1,\ldots,C^{(K)}, \tag{15a}
$$

$$
\{M_{R2}^{(K)}\} = \left\{
\begin{array}{c}
\displaystyle\frac{1}{R!}\int_{-h^{(K)}/2}^{h^{(K)}/2} \sigma_{12}^{(K)}(\zeta^{(K)})^R\left(1 - \frac{\zeta^{(K)}}{R_1^{(K)}}\right)\mathrm{d}\zeta^{(K)} \\[12pt]
\displaystyle\frac{1}{R!}\int_{-h^{(K)}/2}^{h^{(K)}/2} \sigma_{22}^{(K)}(\zeta^{(K)})^R\left(1 - \frac{\zeta^{(K)}}{R_1^{(K)}}\right)\mathrm{d}\zeta^{(K)} \\[12pt]
\displaystyle\frac{1}{R!}\int_{-h^{(K)}/2}^{h^{(K)}/2} \sigma_{32}^{(K)}(\zeta^{(K)})^R\left(1 - \frac{\zeta^{(K)}}{R_1^{(K)}}\right)\mathrm{d}\zeta^{(K)}
\end{array}
\right\} \quad R = 1,\ldots,C^{(K)}, \tag{15b}
$$

$$
\{M_{S3}^{(K)}\} = \left\{
\begin{array}{c}
\displaystyle\frac{1}{S!}\int_{-h^{(K)}/2}^{h^{(K)}/2} \sigma_{13}^{(K)}(\zeta^{(K)})^S\left(1 - \frac{\zeta^{(K)}}{R_1^{(K)}}\right)\left(1 - \frac{\zeta^{(K)}}{R_2^{(K)}}\right)\mathrm{d}\zeta^{(K)} \\[12pt]
\displaystyle\frac{1}{S!}\int_{-h^{(K)}/2}^{h^{(K)}/2} \sigma_{23}^{(K)}(\zeta^{(K)})^S\left(1 - \frac{\zeta^{(K)}}{R_1^{(K)}}\right)\left(1 - \frac{\zeta^{(K)}}{R_2^{(K)}}\right)\mathrm{d}\zeta^{(K)} \\[12pt]
\displaystyle\frac{1}{S!}\int_{-h^{(K)}/2}^{h^{(K)}/2} \sigma_{33}^{(K)}(\zeta^{(K)})^S\left(1 - \frac{\zeta^{(K)}}{R_1^{(K)}}\right)\left(1 - \frac{\zeta^{(K)}}{R_2^{(K)}}\right)\mathrm{d}\zeta^{(K)}
\end{array}
\right\} \quad S = 1,\ldots,C^{(K)}-1, \tag{15c}
$$

$\sigma_{ij}^{(K)}$ being the components of the Cauchy stress tensor.

2.3. Constitutive equations

We assume that the layers of the laminated shell are orthotropic with elastic symmetry with respect to the middle surface and with material principal axes $\hat{\mathbf{i}}_1^{(K)}$, $\hat{\mathbf{i}}_2^{(K)}$ obtained rotating the axes $\hat{\mathbf{e}}_1^{(K)}$, $\hat{\mathbf{e}}_2^{(K)}$ by an arbitrary angle about $\hat{\mathbf{n}}^{(K)}$.

The constitutive equations for the Kth layer are written as:

$$
\sigma_{ij}^{(K)} = C_{ijlm}^{(K)}\varepsilon_{lm}^{(K)} \tag{16}
$$

where $C_{ijlm}^{(K)}$ are the stiffness coefficients of the layer and $\varepsilon_{lm}^{(K)}$ are the components of the infinitesimal strain tensor:

$$\varepsilon_{lm}^{(K)} = \tfrac{1}{2}(\hat{\mathbf{e}}_l^{(K)} \cdot \nabla \mathbf{u}^{(K)} \hat{\mathbf{e}}_m^{(K)} + \hat{\mathbf{e}}_m^{(K)} \cdot \nabla \mathbf{u}^{(K)^T} \hat{\mathbf{e}}_l^{(K)}).$$ (17)

The equations for the terms in the material stiffness matrix and their transformation due to a rotation about $\hat{\mathbf{n}}^{(K)}$ will not be given here, but they can be found in the literature (see, for example, Vinson and Sierakowski, 1987; Graff and Springer, 1991).

By using eqns (4)–(8), (11)–(12), (14)–(17), we obtain the generalized constitutive equations in the following form:

$$\mathbf{N}_i^{(K)} = \sum_{j=1}^{3} \mathbf{C}_{00ij}^{(K)} \mathbf{l}_j^{(K)} + \sum_{R=1}^{C^{(K)}} \sum_{\alpha=1}^{2} \mathbf{C}_{0Ri\alpha}^{(K)} \mathbf{d}_{R\alpha}^{(K)} + \sum_{S=1}^{C^{(K-1)}} \mathbf{C}_{0Si3}^{(K)} \mathbf{d}_{S3}^{(K)},$$ (18a)

$$\mathbf{M}_{R\alpha}^{(K)} = \sum_{i=1}^{3} \mathbf{C}_{R0\alpha i}^{(K)} \mathbf{l}_i^{(K)} + \sum_{T=1}^{C^{(K)}} \sum_{\beta=1}^{2} \mathbf{C}_{RT\alpha\beta}^{(K)} \mathbf{d}_{T\beta}^{(K)} + \sum_{S=1}^{C^{(K-1)}} \mathbf{C}_{RS\alpha 3}^{(K)} \mathbf{d}_{S3}^{(K)}, \quad R = 1,\ldots,C^{(K)},$$ (18b)

$$\mathbf{M}_{S3}^{(K)} = \sum_{i=1}^{3} \mathbf{C}_{S03i}^{(K)} \mathbf{l}_i^{(K)} + \sum_{R=1}^{C^{(K)}} \sum_{\alpha=1}^{2} \mathbf{C}_{SR3\alpha}^{(K)} \mathbf{d}_{R\alpha}^{(K)} + \sum_{U=1}^{C^{(K-1)}} \mathbf{C}_{SU33}^{(K)} \mathbf{d}_{U3}^{(K)}, \quad S = 1,\ldots,C^{(K)}-1,$$ (18c)

where $\mathbf{C}_{VWij}^{(K)}$ are second order tensors defined by the equations:

$$[C_{VWij}^{(K)}]_{lm} = \frac{C_{limj}^{(K)}}{V!W!} \int_{-h^{(K)}/2}^{h^{(K)}/2} \frac{(1-\zeta^{(K)}/R_1^{(K)})(1-\zeta^{(K)}/R_2^{(K)})}{(1-\zeta^{(K)}B_{jj}^{(K)})(1-\zeta^{(K)}B_{mm}^{(K)})} (\zeta^{(K)})^{(V+W)} \, \mathrm{d}\zeta^{(K)}$$

$$B_{11}^{(K)} = 1/R_1^{(K)}, \quad B_{22}^k = 1/R_2^{(K)}, \quad B_{33}^{(K)} = 0.$$ (19)

2.4. Penalty model

Equation (10) sets equal to zero the first variation of the functional of the total potential energy, which is defined on the set K of all admissible displacements for the laminated shell. Let H denote the set of all admissible displacements for the layers, assumed as disconnected from one another. Then K is the subset of H that contains the displacements satisfying the interface constraints (9). We wish to include the constraints (9) into the variational statement (10) by means of the penalty method (Reddy, 1992a, b).

Consider the following functional on H:

$$\Pi_\eta = \Pi + \frac{1}{2\eta} \int_\Omega \sum_{K=1}^{N-1} \Delta \mathbf{u}^{(K)} \cdot \Delta \mathbf{u}^{(K)} \frac{(R_1 - \mathrm{d}^{(K)} - h^{(K)}/2)(R_2 - \mathrm{d}^{(K)} - h^{(K)}/2)}{R_1 R_2} a_1 a_2 \, \mathrm{d}\theta_1 \, \mathrm{d}\theta_2,$$

(20)

where Π is the potential energy of the layers, assumed as disconnected from one another, $\Delta \mathbf{u}^{(K)}$ is the relative displacement defined by eqn (9) and η is a positive parameter.

It can be shown (see, for example, Carey and Oden, 1983; Reddy, 1992a, b) that by considering a sequence of values of η which converges to zero, the result:

$$\lim_{\eta \to 0} \Pi_\eta = \Pi_0,$$ (21)

where Π_0 is the minimum of Π on K. Minimizing Π_η in H, for a small value of η, is usually referred to as the penalty method (Carey and Oden, 1983; Reddy, 1992a, b).

The penaltly technique is particularly convenient in the present case because it allows us to obtain an approximation of the interlaminar stresses (or the Lagrange multipliers), which can be computed from the equations:

$$\lambda_i^{(K)} = \frac{1}{\eta} \Delta u_i^{(K)} \quad K = 1, 2, \ldots, N-1$$ (22)

where

$$\lambda_i^{(K)} = \sigma_{i3}^{(K)}\left(\zeta^{(K)} = \frac{h^{(K)}}{2}\right) = \sigma_{i3}^{(K+1)}\left(\zeta^{(K+1)} = -\frac{h^{(K+1)}}{2}\right). \tag{23}$$

The functional Π_η can be interpreted as the total potential energy of an auxiliary elastic system (penalty model), in which the layers are connected by radial and tangential springs instead of being perfectly bonded. The quantity η is also called the penalty parameter and represents the inverse of the stiffness of these springs in the penalty model.

3. STRESS CALCULATION

We compute the inplane components $(\sigma_{11}^{(K)}, \sigma_{22}^{(K)}, \sigma_{12}^{(K)})$ of the stresses in a generic layer from the constitutive equations,

$$\sigma_{11}^{(K)} = C_{1111}^{(K)}\varepsilon_{11}^{(K)} + C_{1122}^{(K)}\varepsilon_{22}^{(K)} + C_{1133}^{(K)}\varepsilon_{33}^{(K)} + 2C_{1112}^{(K)}\varepsilon_{12}^{(K)}, \tag{24a}$$

$$\sigma_{22}^{(K)} = C_{2211}^{(K)}\varepsilon_{11}^{(K)} + C_{2222}^{(K)}\varepsilon_{22}^{(K)} + C_{2233}^{(K)}\varepsilon_{33}^{(K)} + 2C_{2212}^{(K)}\varepsilon_{12}^{(K)}, \tag{24b}$$

$$\sigma_{12}^{(K)} = C_{1211}^{(K)}\varepsilon_{11}^{(K)} + C_{1222}^{(K)}\varepsilon_{22}^{(K)} + C_{1233}^{(K)}\varepsilon_{33}^{(K)} + 2C_{1212}^{(K)}\varepsilon_{12}^{(K)}. \tag{24c}$$

The strain components $\varepsilon_{ij}^{(K)}$ are computed from eqns (4), (17).

For what concerns transverse stresses $(\sigma_{13}^{(K)}, \sigma_{23}^{(K)}, \sigma_{33}^{(K)})$, we observe that the values of such stresses derived from the strains via constitutive equations, which we denote by

$$\tilde{\sigma}_{13}^{(K)} = 2C_{1313}^{(K)}\varepsilon_{13}^{(K)} + 2C_{1323}^{(K)}\varepsilon_{23}^{(K)}, \tag{25a}$$

$$\tilde{\sigma}_{23}^{(K)} = 2C_{2313}^{(K)}\varepsilon_{13}^{(K)} + C_{2323}^{(K)}\varepsilon_{23}^{(K)}, \tag{25b}$$

$$\tilde{\sigma}_{33}^{(K)} = C_{3311}^{(K)}\varepsilon_{11}^{(K)} + C_{3322}^{(K)}\varepsilon_{22}^{(K)} + C_{3333}^{(K)}\varepsilon_{33}^{(K)} + 2C_{3312}^{(K)}\varepsilon_{12}^{(K)}, \tag{25c}$$

are not continuous across the interfaces of layers with different mechanical properties. On the other hand, the theory formulated in the previous sections gives us an approximation of the effective interlaminar values of transverse stresses. Starting from this consideration, we set in each layer:

$$\sigma_{i3}^{(K)} = \tilde{\sigma}_{i3}^{(K)} + \bar{\sigma}_{i3}^{(K)} \tag{26}$$

where $\bar{\sigma}_{i3}^{(K)}$ are additional stress fields, which give zero stress resultants and moments and let $\sigma_{i3}^{(K)}$ coincide with $\lambda_i^{(K-1)}$ for $\zeta^{(K)} = -h^{(K)}/2$ and with $\lambda_i^{(K)}$ for $\zeta^{(K)} = h^{(K)}/2$ (see eqns (22), (23)). In detail, we express the fields $\bar{\sigma}_{i3}^{(K)}$ in the form:

$$\bar{\sigma}_{13}^{(K)} = \frac{1}{(1 - \zeta^{(K)}/R_1^{(K)})}\left[c_{13}^0 + \sum_{P=1}^{A^{(K)}+1} c_{13}^P(\zeta^{(K)})^P\right], \tag{27a}$$

$$\bar{\sigma}_{23}^{(K)} = \frac{1}{(1 - \zeta^{(K)}/R_2^{(K)})}\left[c_{23}^0 + \sum_{P=1}^{A^{(K)}+1} c_{23}^P(\zeta^{(K)})^P\right], \tag{27b}$$

$$\bar{\sigma}_{33}^{(K)} = c_{33}^0 + \sum_{Q=1}^{B^{(K)}+1} c_{33}^Q(\zeta^{(K)})^Q, \tag{27c}$$

and compute the coefficients $c_{\alpha3}^0$, $c_{\alpha3}^P$, c_{33}^0, c_{33}^Q from the equations:

$$\int_{-h^{(K)}/2}^{h^{(K)}/2} \bar{\sigma}_{\alpha3}^{(K)}\left(1 - \frac{\zeta^{(K)}}{R_1^{(K)}}\right)\left(1 - \frac{\zeta^{(K)}}{R_2^{(K)}}\right)d\zeta^{(K)} = 0, \tag{28a}$$

$$\int_{-h^{(K)}/2}^{h^{(K)}/2} \bar{\sigma}_{\alpha3}^{(K)}\frac{(\zeta^{(K)})^S}{S!}\left(1 - \frac{\zeta^{(K)}}{R_1^{(K)}}\right)\left(1 - \frac{\zeta^{(K)}}{R_2^{(K)}}\right)d\zeta^{(K)} = 0 \quad S = 1, \ldots, A^{(K)} - 1, \tag{28b}$$

$$\bar{\sigma}_{\alpha 3}^{(K)} = \lambda_{\alpha}^{(K-1)} - \tilde{\sigma}_{\alpha 3}^{(K)} \quad \text{for} \quad \zeta^{(K)} = -h^{(K)}/2, \tag{28c}$$

$$\bar{\sigma}_{\alpha 3}^{(K)} = \lambda_{\alpha}^{(K)} - \tilde{\sigma}_{\alpha 3}^{(K)} \quad \text{for} \quad \zeta^{(K)} = h^{(K)}/2, \tag{28d}$$

$$\int_{-h^{(K)}/2}^{h^{(K)}/2} \bar{\sigma}_{33}^{(K)} \left(1 - \frac{\zeta^{(K)}}{R_1^{(K)}}\right)\left(1 - \frac{\zeta^{(K)}}{R_2^{(K)}}\right) d\zeta^{(K)} = 0, \tag{29a}$$

$$\int_{-h^{(K)}/2}^{h^{(K)}/2} \bar{\sigma}_{33}^{(K)} \frac{(\zeta^{(K)})^S}{S!} \left(1 - \frac{\zeta^{(K)}}{R_1^{(K)}}\right)\left(1 - \frac{\zeta^{(K)}}{R_2^{(K)}}\right) d\zeta^{(K)} = 0 \quad S = 1, \ldots, B^{(K)} - 1, \tag{29b}$$

$$\bar{\sigma}_{33}^{(K)} = \lambda_3^{(K-1)} - \tilde{\sigma}_{33}^{(K)} \quad \text{for} \quad \zeta^{(K)} = -h^{(K)}/2, \tag{29c}$$

$$\bar{\sigma}_{33}^{(K)} = \lambda_3^{(K)} - \tilde{\sigma}_{33}^{(K)} \quad \text{for} \quad \zeta^{(K)} = h^{(K)}/2. \tag{29d}$$

It is clear that the stress fields $\sigma_{i3}^{(K)}$ given by eqns (25)–(29) are continuous across the thickness of the laminated shell.

4. FINITE ELEMENT APPROXIMATION

We discretize the middle surface of the laminated shell into a collection of M two-dimensional finite elements. The generalized displacements $(v_i^{(K)}, \phi_{P\alpha}^{(K)}, \phi_{Q3}^{(K)})$ are expressed, over each element, as a linear combination of two-dimensional interpolation functions ψ_L and the nodal values $((v_i^{(K)})_L, (\phi_{P\alpha}^{(K)})_L, (\phi_{Q3}^{(K)})_L)$:

$$v_i^{(K)} = \sum_{L=1}^{NPE} (v_i^{(K)})_L \psi_L, \tag{30a}$$

$$\phi_{P\alpha}^{(K)} = \sum_{L=1}^{NPE} (\phi_{P\alpha}^{(K)})_L \psi_L, \tag{30b}$$

$$\phi_{Q3}^{(K)} = \sum_{L=1}^{NPE} (\phi_{Q3}^{(K)})_L \psi_L, \tag{30c}$$

$$K = 1, 2, \ldots, N; \quad P = 1, \ldots, A^{(K)}; \quad Q = 1, \ldots, B^{(K)}$$

where NPE is the number of nodes per element. By using the isoparametric formulation, we set

$$\theta_\alpha = \sum_{L=1}^{NPE} (\theta_\alpha)_L \psi_L \tag{31}$$

$(\theta_1, \theta_2)_L$ being the global coordinates of the node L.

Setting the first variation of the functional (20) equal to zero and making use of eqns (30), (31), we obtain the equilibrium equations of the discretized penalty model in the following form:

$$\left([K] + \frac{1}{\eta}[K_P]\right)\{U\} = \{Q\}, \tag{32}$$

where $\{U\}$ is the global nodal displacement vector, $[K]$ is the stiffness matrix of the unconstrained problem (layers disconnected) and $1/\eta[K_P]$ is the part of the global stiffness matrix due to the springs connecting the layers in the penalty model. The finite element proposed is characterized by a number $NDF = 3 \cdot N + \Sigma_N^{K=1} (A^{(K)} + B^{(K)})$ of degrees of freedom per node. Hence it leads to a large system of equations, especially when the number of layers is large. However, the computational effort can be reduced by grouping together some layers to form a unique substructure. Moreover, it has to be remarked that the penalty model offers the possibility to easily compute accurate interlaminar stresses and hence it

can be conveniently used when an accurate evaluation of the stress field present in a laminated shell is required.

5. NUMERICAL RESULTS

In order to show the features of the penalty finite element developed herein, we present numerical results for displacements and stresses of simply supported, cross ply laminated spherical shells under uniformly distributed transverse load. The transverse load p is split into two equal parts p^- and p^+ acting at the top and the bottom surface of the shell.

The elastic properties with respect to the principal material axes used in all the examples are:

$$E_1 = 25E_2, \quad E_3 = E_2, \tag{33a}$$

$$G_{13} = G_{12} = 0.5E_2, \quad G_{23} = 0.2E_2, \tag{33b}$$

$$v_{12} = v_{13} = v_{23} = 0.25. \tag{33c}$$

A coordinate system with the origin at the center of the middle surface of the shell is used and the lengths of all the lines of curvature are assumed to be equal $(l_1 = l_2 = l = \text{const})$. Owing to symmetry only a quarter of the shell is modelled. The boundary conditions imposed on the supported sides and on the symmetry axes are:

$$\text{on } \theta_1 = l/2: \quad v_2^{(K)} = v_3^{(K)} = \phi_{P2}^{(K)} = \phi_{Q3}^{(K)} = 0, \tag{34a}$$

$$\text{on } \theta_2 = l/2: \quad v_1^{(K)} = v_3^{(K)} = \phi_{P1}^{(K)} = \phi_{Q3}^{(K)} = 0, \tag{34b}$$

$$\text{on } \theta_1 = 0: \quad v_1^{(K)} = \phi_{P1}^{(K)} = 0, \tag{34c}$$

$$\text{on } \theta_2 = 0: \quad v_2^{(K)} = \phi_{P2}^{(K)} = 0, \tag{34d}$$

$$K = 1, 2, \ldots, N; \quad P = 1, \ldots, A^{(K)}; \quad Q = 1, \ldots, B^{(K)}.$$

The following normalizations are used in presenting the results:

$$(\bar{u}_1, \bar{u}_2) = \frac{E_2}{pl}(u_1, u_2), \quad \bar{u}_3 = \frac{100E_2h^3}{pl^4}u_3, \tag{35a}$$

$$(\bar{\sigma}_{11}, \bar{\sigma}_{22}, \bar{\sigma}_{12}) = \frac{h^2}{pl^2}(\sigma_{11}, \sigma_{22}, \sigma_{12}), \tag{35b}$$

$$(\bar{\sigma}_{13}, \bar{\sigma}_{23}) = \frac{h}{pl}(\sigma_{12}, \sigma_{23}), \tag{35c}$$

$$\bar{\sigma}_{33} = \frac{\sigma_{33}}{p}, \tag{35d}$$

$$\bar{\eta} = \frac{E_2}{l}\eta. \tag{35e}$$

In each of the examples considered we used 16-node cubic finite elements and the Gauss integration formula with four points to compute both the unconstrained stiffness matrix $[K]$ and penalty stiffness matrix $1/\eta[K_p]$. With these quadrature rules we did not observe locking due to shear-bending coupling, extension-bending coupling and the presence of the penalty terms in the global stiffness matrix. In all the examples, we computed stress distributions through the thickness of the shell by post-processing the results of the penalty theory via the procedure described in Section 3.

5.1. Simply supported (0/90) laminated spherical shell under uniform load

This example was chosen to assess the convergence of the penalty finite element model with refinements of the mesh and decreasing values of the penalty parameter η. The center

Table 1. Center deflections and interlaminar stresses for a simply supported (0/90) laminated shell under uniform load. Convergence study of the penalty finite element solutions. $R/l = 1$

↓ Mesh	$l/h = 100$		$\bar{\eta}$			$l/h = 10$		$\bar{\eta}$		
	10^{-1}	10^{-2}	10^{-3}	10^{-4}	10^{-5}	10^{-1}	10^{-2}	10^{-3}	10^{-4}	10^{-5}
2 $\bar{u}_3$	0.0716	0.0719	0.0719	0.0719	0.0719	5.9139	6.0331	6.0705	6.0712	6.0713
× $\bar{\sigma}_{31}$	0.2744	0.0299	0.0286	0.0284	0.0284	0.2513	0.2046	0.1935	0.1927	0.1926
2 $\bar{\sigma}_{32}$	0.2268	0.0158	0.0145	0.0144	0.0144	0.0284	0.0598	0.0493	0.0486	0.0485
4 $\bar{u}_3$	0.0711	0.0719	0.0718	0.0718	0.0718	6.3841	6.0638	6.0712	6.0744	6.0713
× $\bar{\sigma}_{31}$	0.1096	0.0464	0.0385	0.0379	0.0379	1.0922	0.1529	0.1910	0.1896	0.1895
4 $\bar{\sigma}_{32}$	0.3040	0.0319	0.0241	0.0236	0.0235	0.1281	0.1579	0.0473	0.0463	0.0462
6 $\bar{u}_3$	0.0753	0.0718	0.0718	0.0718	0.0718	6.2234	6.0569	6.0704	6.0712	6.0712
× $\bar{\sigma}_{31}$	0.2469	0.0557	0.0365	0.0357	0.0356	0.7471	0.2012	0.1934	0.1892	0.1892
6 $\bar{\sigma}_{32}$	0.1885	0.0414	0.0223	0.0215	0.0214	0.0334	0.0745	0.0481	0.0461	0.0461

Reddy (1984c): $\bar{u}_3 = 0.0718$ for $l/h = 100$, $\bar{u}_3 = 6.054$ for $l/h = 10$.

Table 2. Center deflections and interlaminar stresses for a simply supported (0/90) laminated shell under uniform load. Convergence study of the penalty finite element solutions. $R/l = 10$

↓ Mesh	$l/h = 100$		$\bar{\eta}$			$l/h = 10$		$\bar{\eta}$		
	10^{-1}	10^{-2}	10^{-3}	10^{-4}	10^{-5}	10^{-1}	10^{-2}	10^{-3}	10^{-4}	10^{-5}
2 $\bar{u}_3$	5.5770	5.5457	5.5465	5.5466	5.5467	18.192	18.636	18.676	18.678	18.679
× $\bar{\sigma}_{31}$	16.953	0.2697	0.2614	0.2607	0.2606	0.2766	0.3028	0.2901	0.2891	0.2891
2 $\bar{\sigma}_{32}$	13.649	0.1254	0.1172	0.1165	0.1165	0.2293	0.2575	0.2450	0.2241	0.2440
4 $\bar{u}_3$	5.5262	5.5418	5.5428	5.5427	5.5428	17.935	18.636	18.674	18.678	18.678
× $\bar{\sigma}_{31}$	0.6822	0.2378	0.2216	0.2204	0.2203	0.2627	0.2416	0.2853	0.2838	0.2837
4 $\bar{\sigma}_{32}$	0.7696	0.0943	0.0780	0.0769	0.0768	0.2648	0.1944	0.2403	0.2388	0.2387
6 $\bar{u}_3$	5.5334	5.5417	5.5442	5.5426	5.5427	18.864	18.632	18.674	18.678	18.678
× $\bar{\sigma}_{31}$	0.3983	0.2320	0.2054	0.2043	0.2042	0.7370	0.2744	0.2854	0.2832	0.2830
6 $\bar{\sigma}_{32}$	0.3273	0.0885	0.0621	0.0609	0.0609	2.4784	0.2751	0.2404	0.2382	0.2380

Reddy (1984c): $\bar{u}_3 = 5.5428$ for $l/h = 100$, $\bar{u}_3 = 19.065$ for $l/h = 10$.

deflections and the interlaminar shear stresses computed for different values of R/l and l/h are shown in Tables 1 and 2. The results in terms of center deflections are compared with those obtained by Reddy (1984c). The interlaminar shear stresses σ_{31} were computed at $(\theta_1 = 0.5l, \quad \theta_2 = 0)$ while the interlaminar shear stresses σ_{32} were computed at $(\theta_1 = 0, \theta_2 = 0.5l)$. We set $A = 1$, $B = 0$ in (2) in each of the two layers.

Tables 1 and 2 show that the penalty finite element results in terms of center deflections converge to values close to the solutions given in Reddy (1984c). These were obtained by using a linear inplane displacement field through the whole thickness of the shell (single-layer first order shear deformation theory). Their agreement with the present results was to be expected since it is known that single layer theories accounting for shear deformation lead to satisfactory results in terms of displacements. Tables 1 and 2 also show that the interlaminar stresses given by the present theory converge to constant values as $\bar{\eta}$ converges to zero. The through-the-thickness distributions of the inplane normal stresses σ_{11}, σ_{22} and of the transverse shear stresses σ_{13}, σ_{23} are shown in Figs 2 to 5 for $l/h = 10$; $R/l = 1, 10$ ($R = R_1 = R_2$). These distributions were obtained using a 6×6 uniform mesh of cubic elements over a quarter of the shell and a penalty parameter $\bar{\eta} = 10^{-5}$.

5.2. Simply supported (0/90/0) laminated spherical shell under uniform load

Figures 6 and 7 contain the distributions through laminate thickness of the inplane normal stress σ_{11} and transverse shear stress σ_{13} for the case $(l/R_1 = l/R_2 = 0)$ and for spherical shells characterized by thickness-to-radius ratios $R/l = 10$, $R/l = 1$. The aspect ratio considered is $l/h = 10$. The results for the plate were compared with those obtained
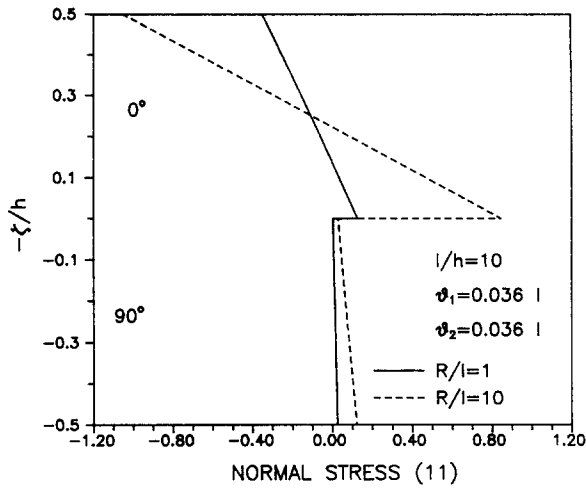
Fig. 2. Through-the-thickness distribution of the inplane normal stress σ_{11} for a simply supported (0/90) laminated spherical shell under double-uniform load.
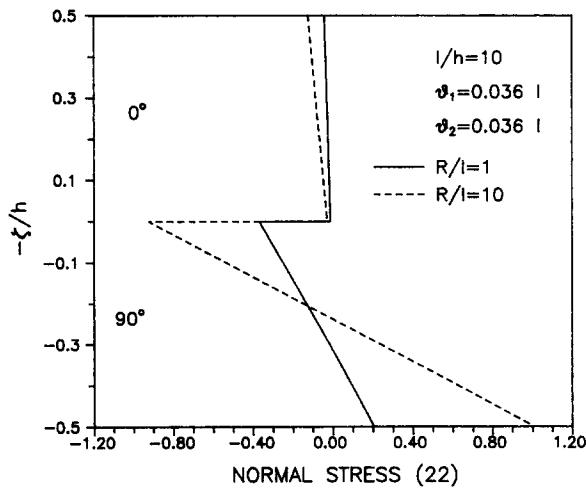

Fig. 3. Through-the-thickness distribution of the inplane normal stress σ_{22} for a simply supported (0/90) laminated spherical shell under double-uniform load.
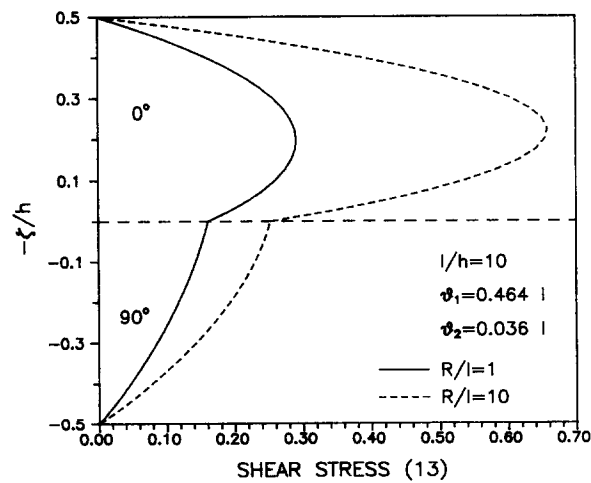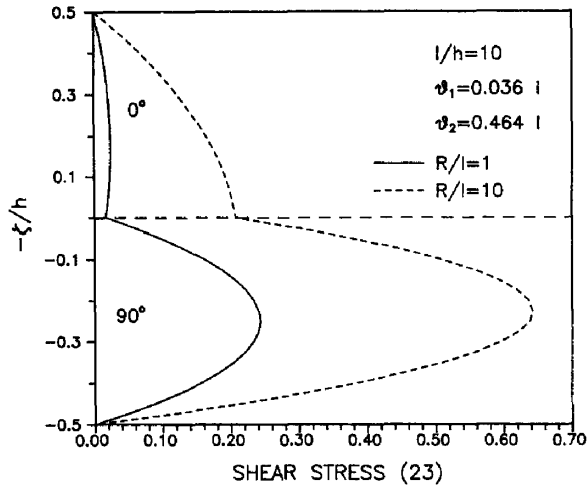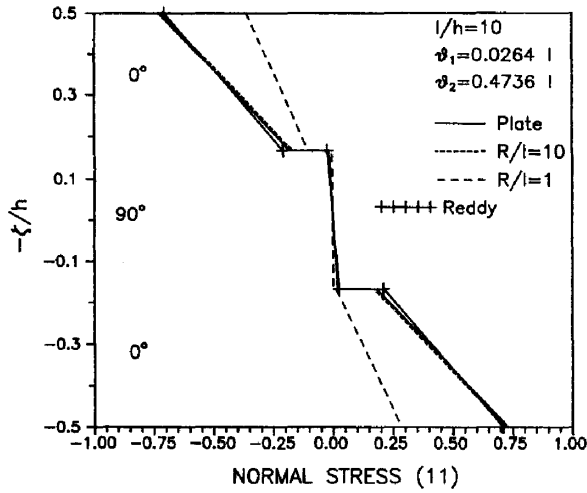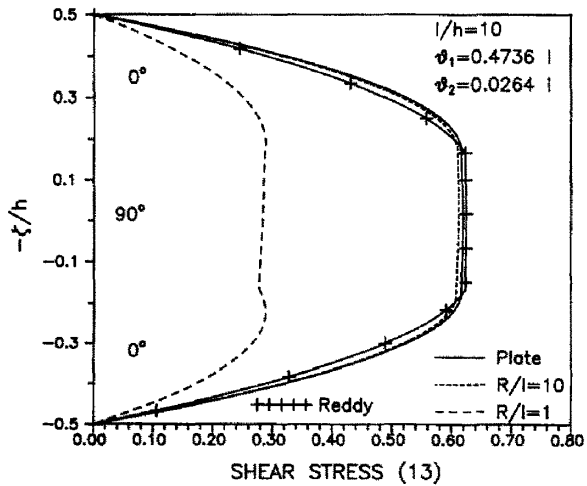

Fig. 4. Through-the-thickness distribution of the transverse shear stress σ_{13} for a simply supported (0/90) laminated spherical shell under double-uniform load.

Fig. 5. Through-the-thickness distribution of the transverse shear stress σ_{23} for a simply supported (0/90) laminated spherical shell under double-uniform load.
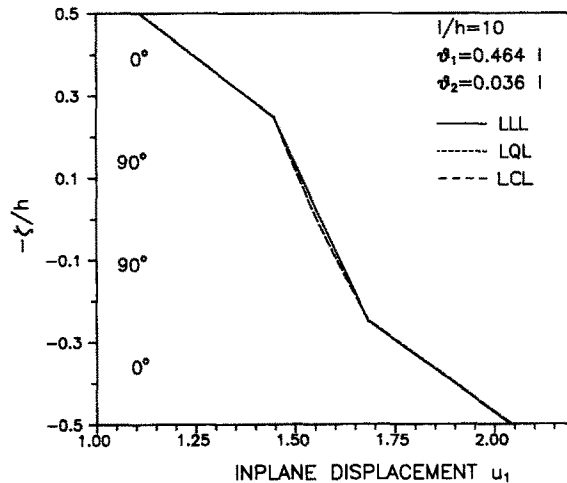

Fig. 6. Through-the-thickness distribution of the inplane normal stress σ_{11} for a simply supported (0/90/0) laminated spherical shell under double-uniform load.

Fig. 7. Through-the-thickness distribution of the transverse shear stress σ_{13} for a simply supported (0/90/0) laminated spherical shell under double-uniform load.

by Reddy *et al.* (1989). For the theory presented in this work, we set $A = 1, B = 0$ in the expression (2) of the displacement field of each layer. We also used the mesh of 6×6 cubic finite elements over a quarter of the laminate and a penalty parameter $\bar{\eta} = 10^{-3}$. It can be observed that the present theory is in close agreement with the General Laminate Plate Theory (GLPT) of Reddy (1987) in the case of the plate.

5.3. *Simply supported (0/90/90/0) laminated spherical shell under double uniform load*

This example was chosen to evaluate the influence of the order of the series expansions (2) of the displacement components on particular displacements and stresses in 0/90/90/0 laminated spherical shells. We set $A = 1, B = 0$ in the two 0 layers and model the two center 90 layers as a unique substructure. In the expression (2) of the displacement field of this substructure we set $B = 0$ and let A vary over 1, 2, 3. A mesh with 6×6 cubic finite elements over a quarter of the laminate is used and the penalty parameter is taken to be $\bar{\eta} = 10^{-3}$.

For $R/l = 1$ and $l/h = 3, 10$ we show, in Figs 8–11, the through-the-thickness distributions of the inplane displacements u_1 and u_2 at particular points. In this and in the subsequent figures, the case $A^{(1)} = A^{(2)} = A^{(3)} = 1$ is denoted by LLL (Linear inplane

Fig. 8. Through-the-thickness distribution of the inplane displacement u_1 for a simply supported (0/90/90/0) laminated spherical shell under double-uniform load, $R/l = 1$.
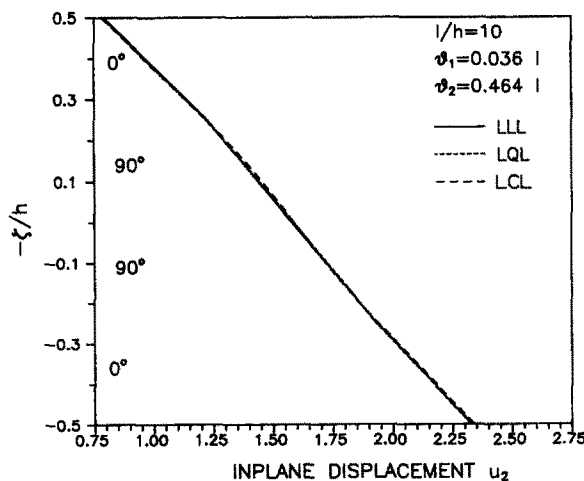
Fig. 9. Through-the-thickness distribution of the inplane displacement u_2 for a simply supported (0/90/90/0) laminated spherical shell under double-uniform load, $R/l = 1$.
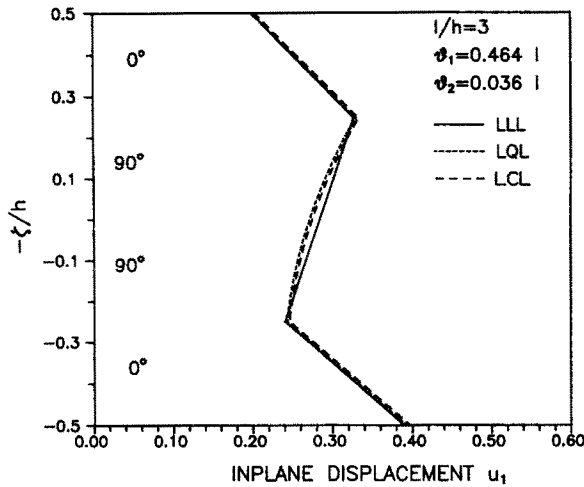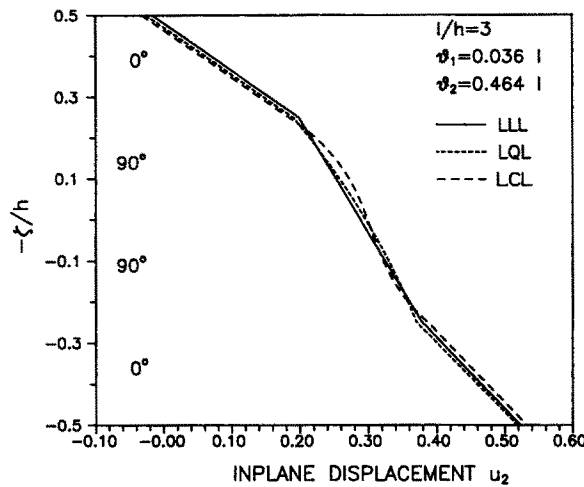
Fig. 10. Through-the-thickness distribution of the inplane displacement u_1 for a simply supported (0/90/90/0) laminated spherical shell under double-uniform load, $R/l = 1$.

Fig. 11. Through-the-thickness distribution of the inplane displacement u_2 for a simply supported (0/90/90/0) laminated spherical shell under double-uniform load, $R/l = 1$.

displacement fields in each of the three layers), the case $A^{(1)} = 1$, $A^{(2)} = 2$, $A^{(3)} = 1$ is denoted by LQL (Linear-Quadratic-Linear inplane displacement fields), the case $A^{(1)} = 1$, $A^{(2)} = 3$, $A^{(3)} = 1$ is denoted by LCL (Linear-Cubic-Linear inplane displacement fields). The distributions of the transverse shear stresses σ_{13} and σ_{23} are shown in Figs 12–15 for $R/l = 1$; $l/h = 3, 10$. For $R/l = 1, l/h = 3$ we also give in Figs 16–18 similar distributions of the normal stresses $\sigma_{11}, \sigma_{22}, \sigma_{33}$. In particular, the distribution of the transverse normal stress σ_{33} was obtained by setting $A = B = 1$ in each layer.

It is evident from Figs 12–17 that the influence of the orders of the series expansions of the displacement components is significant only for thick shells ($l/h < 10$) and that a piecewise linear distribution over the laminate thickness of the inplane displacement components (u_1 and u_2) is sufficient to obtain accurate results for $l/h \geqslant 10$.

6. CONCLUSIONS

The penalty model for laminated composite shells presented in this work can be used to compute both displacements and stresses, with no limitations in the magnitude
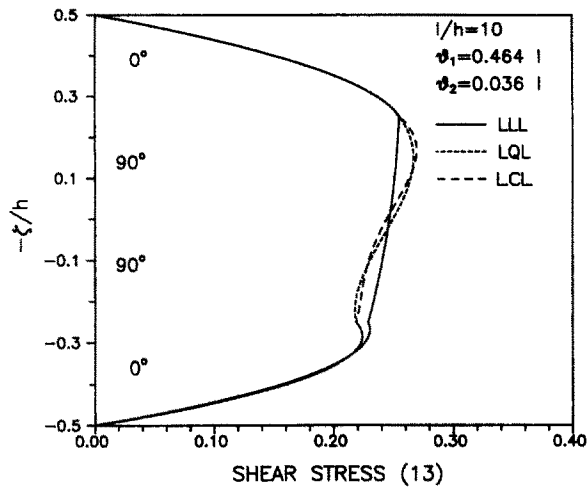
Fig. 12. Through-the-thickness distribution of the transverse shear stress σ_{13} for a simply supported (0/90/90/0) laminated spherical shell under double-uniform load, $R/l = 1$.
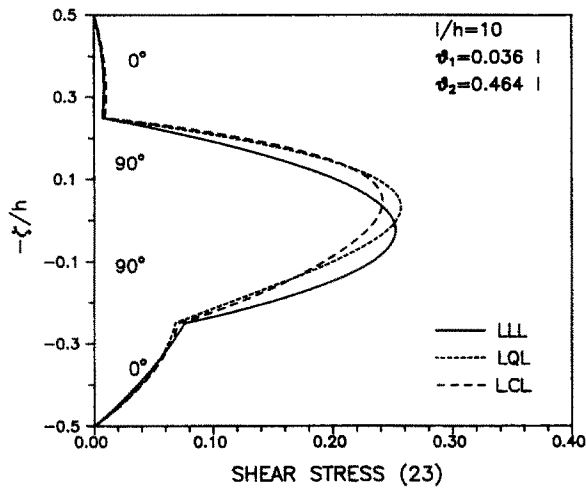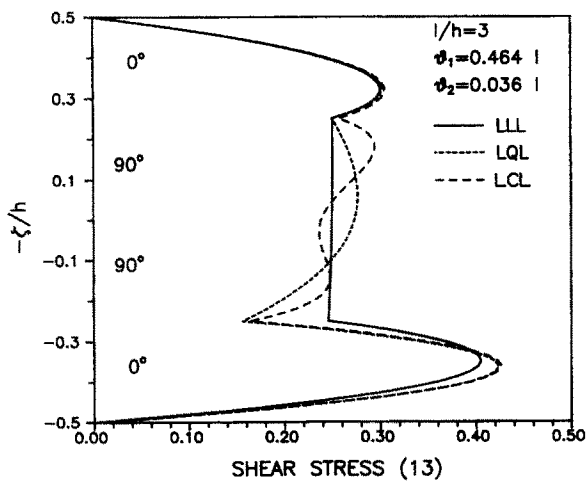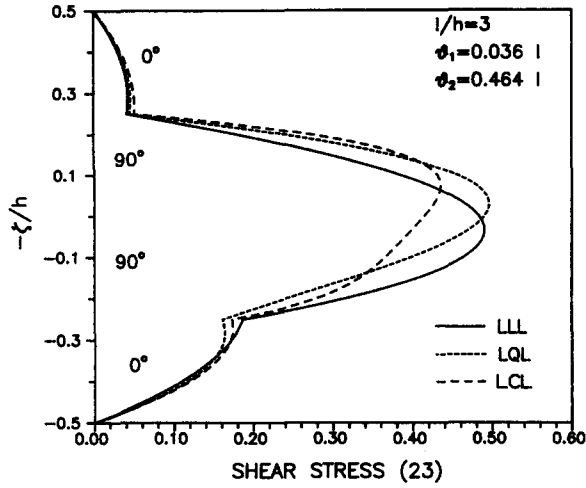
Fig. 13. Through-the-thickness distribution of the transverse shear stress σ_{23} for a simply supported (0/90/90/0) laminated spherical shell under double-uniform load, $R/l = 1$.

Fig. 14. Through-the-thickness distribution of the transverse shear stress σ_{13} for a simply supported (0/90/90/0) laminated spherical shell under double-uniform load, $R/l = 1$.

Fig. 15. Through-the-thickness distribution of the transverse shear stress σ_{23} for a simply supported (0/90/90/0) laminated spherical shell under double-uniform load, $R/l = 1$.
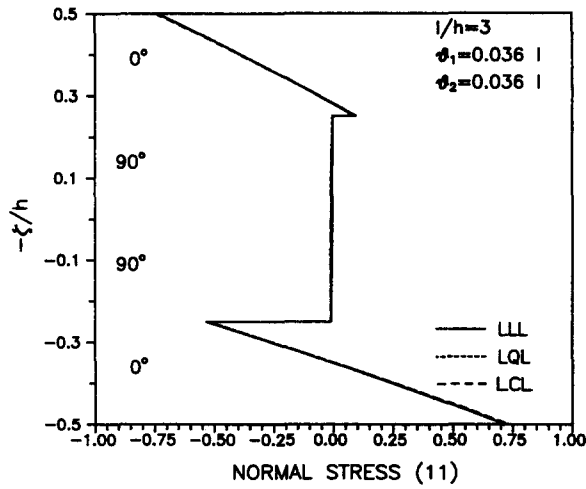

Fig. 16. Through-the-thickness distribution of the inplane normal stress σ_{11} for a simply supported (0/90/90/0) laminated spherical shell under double-uniform load, $R/l = 1$.
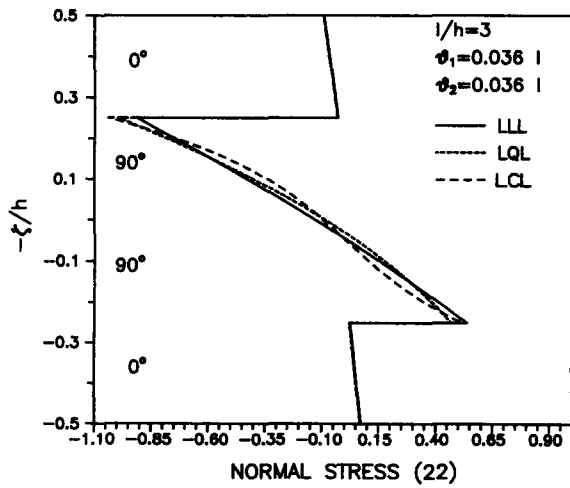

Fig. 17. Through-the-thickness distribution of the inplane normal stress σ_{22} for a simply supported (0/90/90/0) laminated spherical shell under double-uniform load, $R/l = 1$.
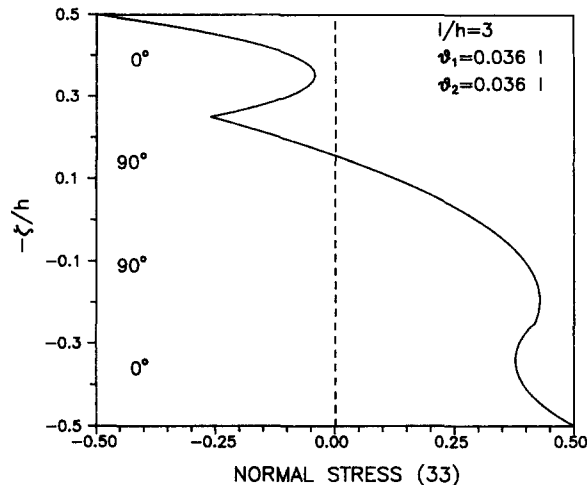
Fig. 18. Through-the-thickness distribution of the transverse normal stress σ_{33} for a simply supported (0/90/90/0) laminated spherical shell under double-uniform load, $R/l = 1$.

of the thickness-to-radius and thickness-to-length ratios. The flexibility of the adopted displacement representation allows one to fit the theory to the problem to be solved in an optimal way. Furthermore, interlaminar stresses are easy to compute, since they represent the Lagrange multipliers, which can be computed in a direct way. The numerical results obtained by the finite element method show good convergence of the discretized penalty model with mesh refinements and decreasing value of the penalty parameter. The agreement between the finite element results and the solutions given by Reddy (1984c) is good. Due to the use of the penalty method to enforce the bonding constraint between layers, the proposed theory can be easily extended to relax this constraint and include delamination effects.

REFERENCES

Ascione, L. and Fraternali, F. (1990). On the mechanical behaviour of laminated curved beams: a simple model which takes into account the warping effects. *Rend. Mater. Acc. Lincei* **1**, 223–233.
Ascione, L. and Fraternali, F. (1992). A penalty model for the analysis of laminated curved beams. *Comput. Struct.* **45**, 985–999.
Bhimaraddi, A., Car, A. J. and Moss, P. J. (1989). Generalized finite element analysis of laminated curved beams with constant curvature. *Comput. Struct.* **31**, 309–317.
Carey, G. F. and Oden, J. T. (1983). *Finite Elements: A Second Course.* Prentice-Hall, Englewood Cliffs, New Jersey.
Christensen, R. M., Lo, K. H. and Wu, E. M. (1977). A high-order theory of plate deformation—part 2: laminated plates. *J. Appl. Mech.* **44**(4), 669–676.
Dym, C. L. (1974). *Introduction to the Theory of Shells.* Pergamon Press, Oxford.
Graff, E. and Springer, G. S. (1991). Stress analysis of thick, curved composite laminates. *Comput. Struct.* **38**, 41–55.
Hildebrand, F. B., Reissner, E. and Thomas, G. B. (1949). Notes on the foundations of the theory of the small displacements of orthotropic shells. *NACA TN* **1833**.
Hinrichsen, R. L. and Palazzotto, A. N. (1986). The non linear finite element analysis of the thick composite plates using cubic spline functions. *AIAA Jl* **24**, 1836–1842.
Malkus, D. S. and Hughes, T. J. R. (1978). Mixed finite element methods—reduced and selective integration techniques: a unification of concepts. *Comput. Meths. Appl. Mech. Engng* **15**, 63–81.
Murakami, H. (1984). Laminated composite plate theories with improved inplane responses. *ASME Pressure Vessels and Piping Conf.* pp. 257–263.
Murthy, M. V. V. (1981). An improved transverse shear deformation theory for laminated anisotropic plates. *NASA Technical Paper* **1903**.
Naghdi, P. M. (1957). The effect of transverse shear deformation on the bending of elastic shells of revolution. *Quart. Appl. Mech.* **15**(1), 41–52.

Naghdi, P. M. (1972). The theory of shells and plates. *Handbuch der Physik*, Vol. VIa/2, Springer, Berlin.

Reddy, J. N. (1984a). *Energy and Variational Method in Applied Mechanics*. John Wiley, New York.

Reddy, J. N. (1984b). A simple higher-order theory for laminated composite plates. *J. Appl. Mech.* **51**, 745–752.

Reddy, J. N. (1984c). Exact solutions of moderately thick laminated shells. *J. Engng Mech.* **110**, 794–809.

Reddy, J. N. (1987). Generalization of two-dimensional theories of laminated composite plates. *Commun. Appl. Numer. Meth.* **3**, 173–180.

Reddy, J. N. (1992a). *An Introduction to the Finite Element Method*, 2nd Edn. McGraw-Hill, New York.

Reddy, J. N. (1992b). *Applied Functional Analysis and Variational Methods in Engineering*. Krieger, Melbourne, FL.

Reddy, J. N., Barbero, E. J. and Teply, J. L. (1989). A plate bending element based on a generalized laminate plate theory. *Int. J. Numer. Meth. Engng* **28**, 2275–2292.

Reddy, J. N. and Liu, C. F. (1985). A higher order shear deformation theory of laminated elastic shells. *Int. J. Engng Sci.* **23**(3), 319–330.

Reddy, J. N. and Barbero, E. J. (1990). General two-dimensional theory of laminated cylindrical shells. *AIAA Jl* **28**, 544–553.

Reddy, J. N. and Chandrasekhara, K. (1987). Recent advances in the non linear analysis of laminated composite plates and shells. *Shock Vibr. Dig.* **19**(4), 3–9.

Sreenivas, S. (1973). A refined analysis of composite laminates. *J. Sound Vibr.* **30**(4), 495–507.

Tralli, A., Laudiero, F. and Savoia, M. (1990). A model for the analysis of laminated composite beams. *Proc. X National Congress AIMETA*, Vol. 1, 285–289, Pisa.

Vinson, J. R. and Sierakowski, R. L. (1987). *The Behaviour of Structures Composed of Composite Materials*. Martinus Nijhoff Publ., Dordrecht.

Yuan, F. G. and Miller, R. E. (1989). A new finite element for laminated composite beams. *Comput. Struct.* **31**, 737–745.